Electrochemical Reduction of the Antitumour Anthrapyrazole CI-941: Mechanism of Formation and Isolation of the Leuco Form

Agnès Anne *
Laboratoire de Chimie Analytique (UA CNRS 484), Faculté Pharmacie, Université Paris V, 4 Ave Observatoire, 75270 Paris Cedex 06, France
Jacques Moiroux *
Laboratoire de Chimie Analytique, Université de Picardie, 3 Pl. L. Dewailly, 80037 Amiens Cedex, France

The title compound undergoes two successive one-electron reductions in the aprotic solvent DMF and an apparent one-step two-electron reduction in the presence of proton donors. Both the leuco form, resulting from the addition of two electrons and two protons, and the product of its hydrolysis in acidic media, have been isolated. All of the observed reactions proceed according to thermodynamic and kinetic parameters (redox potentials, pK_as and rate constants) which are quantitatively analysed.

Since dose-related cardiotoxicity[1] has been the principal clinical limitation of the anthracycline doxorubicin,[2] the most widely prescribed anticancer drug, many efforts have been devoted to developing alternative and less toxic synthetic agents. Among the more promising types of drugs are the anthrapyrazoles.[3]

A preliminary polarographic study[3] suggested that anthrapyrazoles are appreciably less readily reduced than anthracyclines and, consequently, are probably not involved in the same enzymatically driven redox processes which generate free radicals and are believed to be lethal to cardiac cells.[4] However, that does not exclude the possibility of metabolic activation of the drug, perhaps *via* reductive processes.

This paper deals with the mechanism of the reduction of the anthrapyrazole anticancer agent, CI-941, in moderately acidic media and the isolation, identification, and stability of its leuco product. The reducing reagent is a cathode whose advantages derive from the possibility of varying continuously the driving force of the reduction by means of the electrode potential. In the present work, the electrode potential[5] was adjusted so that the reduction could always proceed under the mildest conditions and, therefore, the kinetics of the overall reaction could be easily measured by the electrode current flow.

Hereafter, the parent compound will be referred to as **An** regardless of the solution acidity, since there is no reason to assume that the protonation of the distal amino groups of the side chains can affect the redox properties of the anthrapyrazole chromophore.

Cyclic Voltammetry.—Cyclic voltammetry of a so-called solution of neutralized **An** in DMF (see Experimental Section: *Electrochemistry*) shows that **An** undergoes a reversible one-electron reduction regardless of the potential sweep rate v, with the corresponding standard redox potential E_1^0 being $-1\,305 \pm 5$ mV.

$$\mathbf{An} + e \overset{E_1^0}{\rightleftharpoons} \mathbf{An}^{\bullet -}$$

Scheme 1.

A second one-electron addition occurs at *ca.* $-1\,900$ mV. This second process is irreversible even at $v = 200$ V s^{-1}, with the consecutive protonation (Scheme 3) of the strong base $\mathbf{An}^{2-}$ by weak proton donors TH (such as water) being fast.

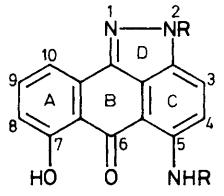

An

R = CH_2-CH_2-NH-CH_2-CH_2-OH or
R = CH_2-CH_2-NH_2^+-CH_2-CH_2-OH,Cl^-

$$\mathbf{An}^{\bullet -} + e \overset{E_2^0}{\rightleftharpoons} \mathbf{An}^{2-}$$

Scheme 2.

$$\mathbf{An}^{2-} + TH \overset{\text{fast}}{\rightleftharpoons} \mathbf{AnH}^- + T^-$$

Scheme 3.

Therefore, the value of E_2^0 cannot be determined by means of cyclic voltammetry; it can only be ascertained that $E_2^0 < -1\,900$ mV. The reverse sweep exhibits a peak due to the oxidation of $\mathbf{AnH}^-$ at a potential that does not differ appreciably from E_1^0.

The absorption spectra of $\mathbf{An}^{\bullet -}$ and $\mathbf{AnH}^-$ obtained by means of spectroelectrochemistry are reproduced in Figure 1. The absorption spectrum of $\mathbf{An}^{\bullet -}$ in DMF and that of its protonated form $\mathbf{AnH}^{\bullet}$ produced by means of pulse radiolysis in buffered (pH 7.0) aqueous media,[6] exhibit very similar features especially at wavelengths greater than 400 nm. Electrochemical oxidation at -730 mV of either $\mathbf{An}^{\bullet -}$ or $\mathbf{AnH}^-$ regenerates the spectrum of **An**.

In buffered acidic medium (42 TEA·HCl, 8 mmol dm^{-3} TEA, *i.e.* pH^{DMF} is *ca.* 8.3 since pK_a^{DMF}TEA·HCl is *ca.* 9.0),[7] an apparent one-step reversible two-electron reduction of **An** occurs at slow v ($v = 0.2$ Vs^{-1}) as shown by the system of peaks P_{c1} and P_{a1} appearing in Figure 2(*a*).

When the acidity of the medium is weaker, the cathodic signal actually consists of two overlapping peaks indicating that two processes compete under those conditions. The first peak, *i.e.* the one appearing at the less negative potential, reveals the occurrence of the one-step, two-electron reduction of a certain amount of **An** which produces $\mathbf{AnH}^-$. The second peak corresponds to the one-electron reduction of the remaining

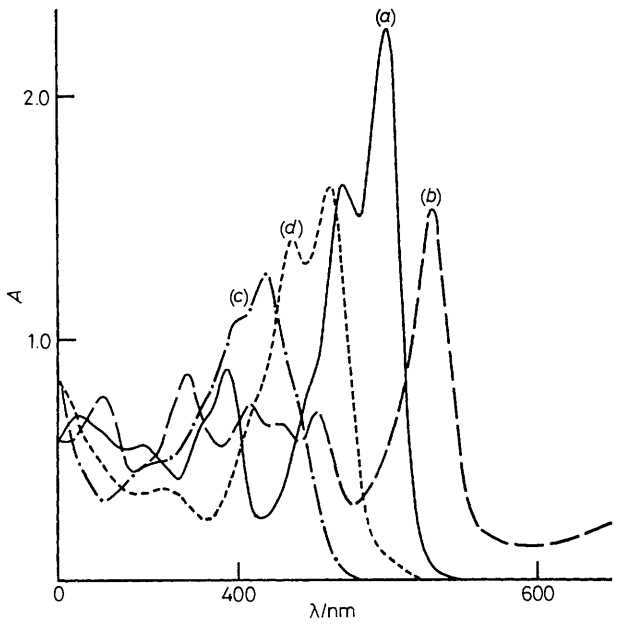

Figure 1. Controlled-potential electrolysis of 1.0 mmol dm^{-3} **An** in DMF (0.05 mol dm^{-3} Et_4NCl) followed by means of u.v.–vis. spectrophotometry. Cell thickness: 0.2 cm. Curve (*a*) (——) absorption spectrum of **An**. Curves (*b*) (— —) and (*c*) (— · —) after exhaustive electrolyses in the presence of 2.5 mmol dm^{-3} Et_4NOH at a gold-grid cathode (cell for spectroelectrochemistry) at −1 350 ($\mathbf{An}^{\bullet -}$) and −1 950 mV ($\mathbf{AnH}^-$) respectively. Curve (*d*) (– – – –) after electrolysis at −1 180 mV (mercury-pool electrode) in the presence of 0.05 mol dm^{-3} TEA·HCl and 6.3 mmol dm^{-3} HCl.

amount of **An** thus producing $\mathbf{An}^{\bullet -}$ the reduction of which can be observed at a much more negative potential. Therefore, the possibility of obtaining an apparent one-step, two-electron reduction (Scheme 6) arises from the protonation of $\mathbf{An}^{\bullet -}$ according to the sequence of Schemes 1, 4, and 5, Schemes 4 and 5 being as follows:[8]

$$\mathbf{An}^{\bullet -} + \text{TEA·H}^+ \rightleftharpoons \mathbf{AnH}^{\bullet} + \text{TEA}$$

Scheme 4.

$$\mathbf{An}^{\bullet -} + \mathbf{AnH}^{\bullet} \rightleftharpoons \mathbf{AnH}^- + \mathbf{An}$$

Scheme 5.

$$\mathbf{An} + \text{H}^+ + 2\,\text{e} \overset{E_6^{0'}}{\rightleftharpoons} \mathbf{AnH}^-$$

Scheme 6.

When the acidity of the medium is greater, the two-electron reduction becomes irreversible due to the protonation of $\mathbf{AnH}^-$ which yields a species $\mathbf{AnH}_2$.

$$\mathbf{AnH}^- + \text{TEA·H}^+ \underset{k_{-7}}{\overset{k_7}{\rightleftharpoons}} \mathbf{AnH}_2 + \text{TEA}$$

Scheme 7.

$\mathbf{AnH}_2$ is oxidizable only at the potential of the anodic peak noted P_{a2} in Figure 2(*b*).

At pH^{DMF} 8.3, a rather unusual behaviour is observed when v varies. The reversibility of the system of peaks P_{c1} and P_{a1} decreases with increasing v, *i.e.* the height of peak P_{a1} decreases in favour of peak P_{a2} as can be seen in Figure 2(*a*) and (*b*). Simultaneously the peak potential E_{pc1} shifts towards the negative. Such behaviour is typical of a mechanism consisting of the reversible electrochemical process, Scheme 6 followed by the

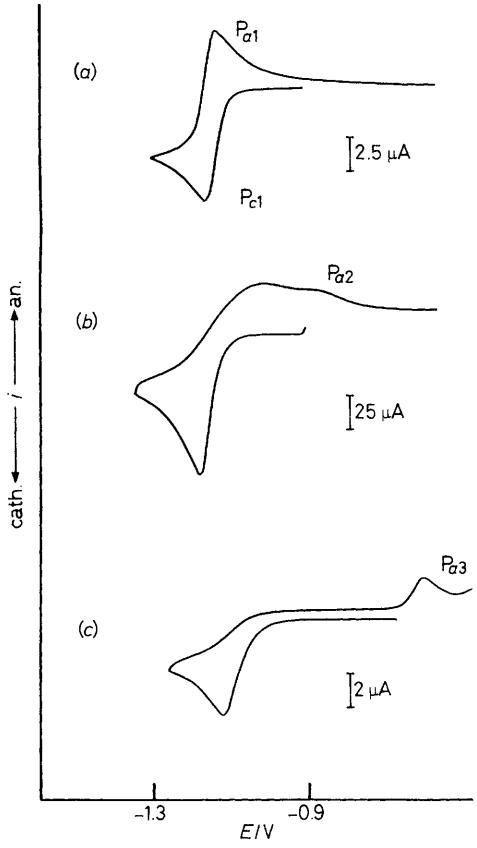

Figure 2. Cyclic voltammetry at the hanging-mercury-drop electrode in buffered acidic DMF. (*a*) v = 0.2 V s^{-1} and (*b*) v = 20 V s^{-1}, in the presence of 0.1 mol dm^{-3} Et_4NCl, 42 TEA·HCl and 8 mmol dm^{-3} TEA, [**An**] 0.82 mmol dm^{-3}. (*c*) v = 1 V s^{-1}. in the presence of 0.2 mol dm^{-3} Et_4NCl, 2 mmol dm^{-3} HCl, [**An**]: 0.22 mmol dm^{-3}.

reversible proton transfer, Scheme 7, the latter obeying pseudo-first-order kinetics in buffered media. The theoretical treatment of that mechanism is given in the literature.[9] The experimental E_{pc1} *vs.* log v plot correlates well with the theoretical working curve when the kinetic parameter $p/v^{\frac{1}{2}} = K_7([\text{TEA·H}^+]/[\text{TEA}]) \times (2F/RT)^{\frac{1}{2}} \times [k_7(\text{TEA·H}^+) + k_{-7}(\text{TEA})]^{-\frac{1}{2}}$ is 0.707 at 25 °C [Figure 3(*a*)]. The proton transfer Scheme 7 probably being fast,[10] it seems reasonable to assume that k_7 approaches the diffusion limit, *i.e.* 10^8 dm^3 mol^{-1} $s^{-1} \leqslant k_7 \leqslant 10^{10}$ dm^3 mol^{-1} s^{-1}. Therefore, $30 \leqslant K_7 \leqslant 300$. Then good estimates of pK^{DMF}_{a,AnH_2} and the apparent standard redox potential $E_6^{0'}$ can be calculated: $pK^{DMF}_{a,AnH_2} = 11.0 \pm 0.5$ and $E^0_{6pH(DMF)\ 8.3} = -1\,215 \pm 15$ mV. pK^{DMF}_{a,AnH^-} can also be estimated since $pK^{DMF}_{a,AnH^-} = (2E_6^0 - E_1^0 - E_2^0)/60$. As $E_2^0 < -1\,900$ mV, $pK^{DMF}_{a,AnH^-} > 21$, *i.e.* $\mathbf{An}^{2-}$ is a very strong base in accord with the observed rapidity and irreversibility of Scheme 3.

The following changes in the features of the voltammogram are observed with increasing acidity of the medium, v being kept constant. Peak P_{a2} develops, while P_{a1} vanishes, but never reaches a height equal to that of P_{c1}. When $pH^{DMF} < 6$, it is peak P_{a2} which vanishes in favour of the development of a new anodic peak noted P_{a3}. When P_{a3} is the sole observable anodic peak [see Figure 2(*c*)] its height is also much smaller than that of P_{c1} and decreases with increasing acidity. Therefore, P_{a3} corresponds to the oxidation of a species called $\mathbf{1AnH}_2$ the formation of which seems to be acid-catalysed and which is unstable on the time scale of cyclic voltammetry. It undergoes a spontaneous transformation, also accelerated in acidic media, which produces a non-electroactive species that will be referred to as $\mathbf{LAnH}_2$ further in the text.

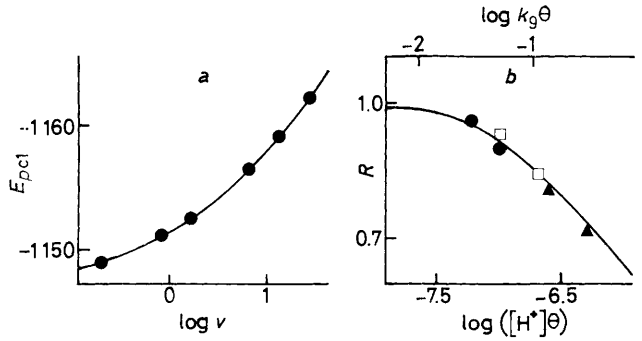

Figure 3. Electrochemical reduction of **An** in buffered acidic DMF at the hanging-mercury-drop, at 25 °C. (*a*) Cyclic voltammetry. Variation of the peak potential E_{pc1} with log *v*: ●, in the presence of 0.1 mol dm^{-3} Et_4N·Cl, 42 TEA·HCl and 8 mmol dm^{-3} TEA, **An** concentration: 0.82 mmol dm^{-3}. The solid line represents the theoretical variation for an *ec* mechanism when the kinetic parameter $p/v^{\frac{1}{2}}$ (see the text) = 0.707. (*b*) Double potential step chronoamperometry from −530 to −1 250 mV and back at time θ. Variation of the current ratio *R* with log ([H$^+$]θ) in the presence of 0.2 mol dm^{-3} Et_4N·Cl and various HCl concentrations: ● 2, □ 4, ▲ 10 mmol dm^{-3} HCl, [**An**] 0.22 mmol dm^{-3}. The solid line represents the theoretical variation for an *ec* mechanism when the kinetic parameter $k_9\theta$ is (5 ± 1) × 10^5 [H$^+$]θ.

$$\mathbf{AnH_2} \longrightarrow \mathbf{1AnH_2}$$

Scheme 8.

$$\mathbf{1AnH_2} \xrightarrow{k_9} \mathbf{LAnH_2}$$

Scheme 9.

The use of a third sweep towards negative potentials provides evidence that the oxidation occurring at the level of peak P_{a2} regenerates **An** to the amount which is in agreement with the relative height of the peak, whereas no regeneration can be obtained at the level of peak P_{a3}.

Double potential step chronoamperometry can be used for studying the kinetics of the mechanism consisting of Schemes 6–8 which are fast and irreversible in sufficiently acidic media, and Scheme 9 which can be partially outrun in the time scale of the experiment. The pH^{DMF} was controlled by the ratio [HCl]: [Cl$^-$], the pK_a^{DMF} of HCl being 3.4.[7] At time zero, the potential was stepped from −530 mV (a potential positive of E_{pa3}) to −1 250 mV (negative of E_{pc1}) and back at time θ. The ratio $i_{(2\theta)}$:$i_{(\theta)}$ was measured at various θ and pH values, $i_{(2\theta)}$ being the anodic current at time 2θ and $i_{(\theta)}$ being the cathodic current at time θ. The corresponding rate constant k_9 = (5 ± 1) × 10^5(H$^+$) s^{-1} can then be derived from the fitting between the experimental data and a theoretical curve which can be deduced from Ref. 11 [Figure 3(*b*)]. The pH^{DMF} dependence of k_9 shows that the reaction in Scheme 9 is acid-catalysed.

$LAnH_2$ *Identification.*—**$LAnH_2$** is quantitatively produced by means of preparative electrolysis under carefully controlled acidic conditions (see the Experimental section). The final absorption spectrum is reproduced in Figure 1 and is quite similar to those reported for the stable leuco tautomers obtained by reduction of 1,4-bis(alkylamino)anthraquinones.[12] Spectroscopic analysis of purified **$LAnH_2$** demonstrates that this compound exists as the 3,4-dihydro–**An** tautomer (see Scheme 10). In particular, the ^{1}H n.m.r. spectrum lacks the two aromatic doublet resonances, assigned to the C-3-H and C-4-H protons in **An**; this disappearance, coupled with the appearance of two additional methylene groups at δ 3.33, demonstrates the loss of aromaticity in the ring. The same trends were also reported for leuco forms of the anthraquinone series.[12,13] The presence of the C-5 proximal amine proton is evidenced by the observation of a characteristic downfield triplet at δ 10.91 (in the ^{1}H n.m.r. spectrum of **An**, the corresponding signal occurs at δ 8.9); this nitrogen proton forms an intramolecular hydrogen bond with the C-6 carbonyl group, as indicated by its absorption position, and is coupled to the adjacent methylene group (*J* 6 Hz), as confirmed by decoupling experiment.

Hydrolysis of **$LAnH_2$**.—The spectrophotometric behaviour of **$LAnH_2$** in aqueous media (Figure 4) shows that this compound can be protonated at pH <2 and that this protonation is reversible (Scheme 11):

$$\mathbf{LAnH_2} + H^+ \overset{K_a}{\rightleftharpoons} \mathbf{LAnH_3}^+$$

Scheme 11.

As can be seen in Figure 4 the protonation induces hypsochromic shifts of 16 and 18 nm of the bands at 451 and 429 nm respectively. However, **$LAnH_3^+$** is unstable and undergoes a spontaneous transformation which can be followed spectrometrically. Three isosbestic points appear at 309, 331, and 402 nm, proving that this transformation of **$LAnH_3^+$** produces only one species absorbing at wavelengths greater than 300 nm, this species resulting from the cleavage of a side chain (see further):

$$\mathbf{LAnH_3}^+ \xrightarrow{k_{11}} \mathbf{P} + \text{side chain}$$

Scheme 12.

The variation of [P] was monitored at both 394 and 434 nm. Assuming, as seems reasonable, that the reaction in Scheme 12 obeys first-order kinetics, it follows:

$$d(P)/dt = [k_{11}[H^+]/(K_a + [H^+])]([\mathbf{LAnH_2}] + [\mathbf{LAnH_2}^+]) \quad (1)$$

$$\text{and } \ln (A_t - A_\infty) = -(k_{11}[H^+]/(K_a + [H^+])t + \ln (A_0 - A_\infty) \quad (2)$$

A_0, A_t, and A_∞ being the absorbances of the solution at times zero, *t*, and at the completion of the transformation respectively. Kinetic data collected at various [H$^+$] are in agreement with equation (2) provided that pK_a = 0.6 ± 0.1 and k_{11} = (1.1 ± 0.2) × 10^{-3} s^{-1} at 32 °C as appears in the insert of Figure 4.

^{1}H N.m.r. and mass spectroscopic data for purified **P** establish that this compound in the monohydroxy derivative of **$LAnH_2$**, resulting from the hydrolysis of the aminoethylamino side chain at position 5. Further analysis of the ^{1}H n.m.r. spectrum is consistent with the assignment to this compound of a 3,4-dihydro leuco structure (see Scheme 10): the three aromatic protons of the A-ring remain present but appear in an AMX system (δ 7.07—7.81) instead of an A_2X system as for **An** and its leuco form **$LAnH_2$**; in addition to the methylene resonances of the N-2 linked side chain, the upfield region exhibits a set of triplets at δ 3.41 and 2.98, associated with the two coupled methylene groups (*J* 7 Hz) of the C-ring. The least shielded resonance is found in the appropriate position for assignment as the C-3 methylene group (δ 3.33 in **$LAnH_2$**). The C-4 methylene group appears at a position (δ 2.98) close to that of the corresponding methylene of leuco-1,4-dihydroxyanthracenediones (δ *ca.* 3.05),[12–14] which were shown to possess a carbonyl functionality adjacent to the cyclic methylene groups. This chemical shift is also in agreement with that of the methylene protons (δ 2.88) of a closely related compound, leuco-1-butylamino-4-hydroxyanthraquinone which was assigned an unsymmetrical 4,9-diketo structure.[15]

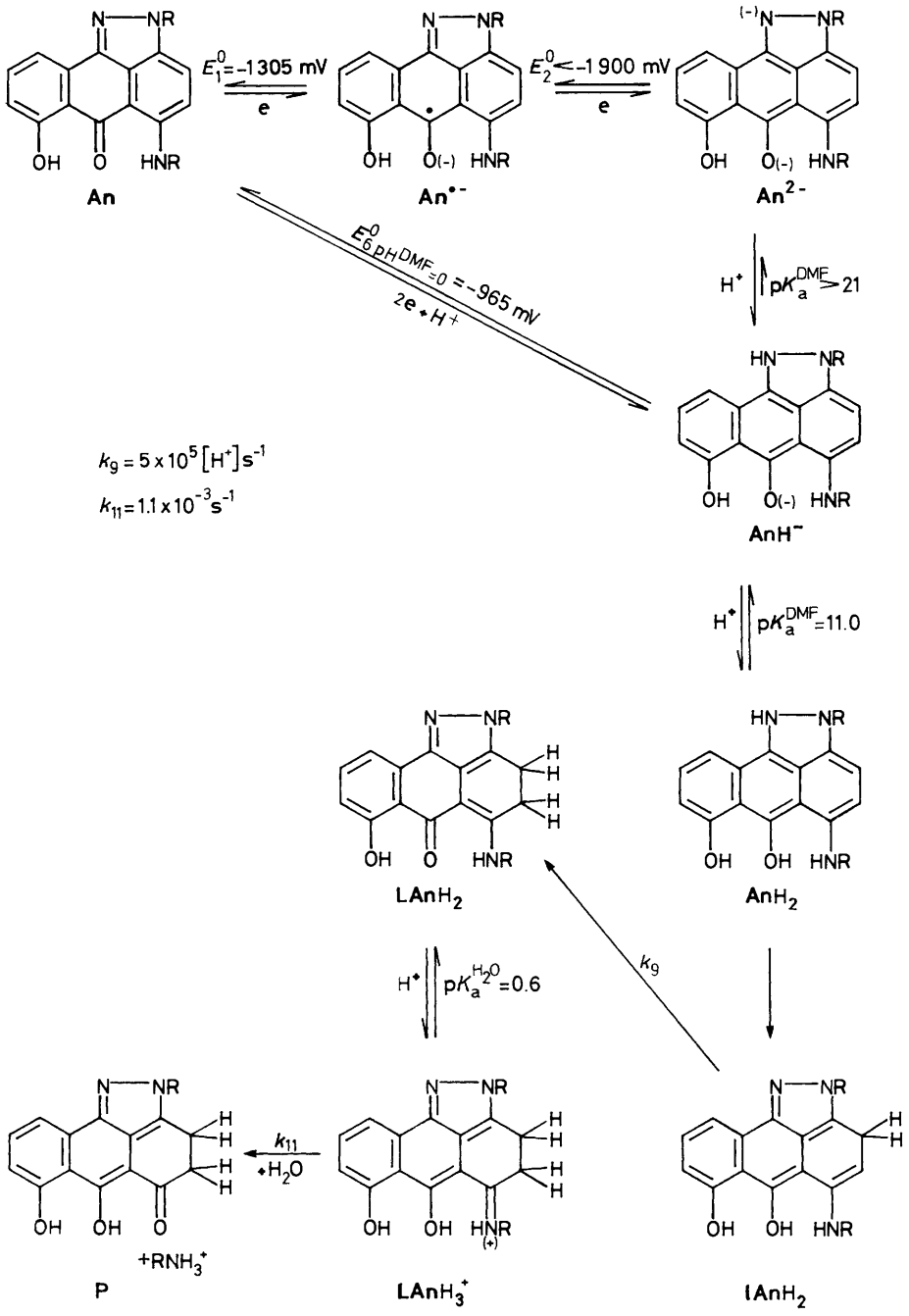

Scheme 10. Reduction of the parent compound in the presence of proton donors: reaction pathway. Electrochemical characterizations: $\mathbf{An}^{\bullet -}$, $\mathbf{AnH}^-$, and $\mathbf{AnH_2}$. Spectrophotometric characterizations: $\mathbf{An}^{\bullet -}$, $\mathbf{AnH}^-$, and $\mathbf{LAnH_3}^+$. $\mathbf{LAnH_2}$ and **P** have been prepared, isolated and identified. $\mathbf{An}^{2-}$ can exist in resonant forms.

Reaction Pathway.—In aprotic DMF, the reduction proceeds through two well-separated one-electron steps in agreement with the usual behaviour of quinonoid compounds.

All the information collected in the present work concerning the reductive reaction pathway in the presence of proton donors is summarized and reported in Scheme 10. Indeed, the anionic species $\mathbf{An}^{\bullet -}$ and $\mathbf{An}^{2-}$ can exist in resonant forms. $\mathbf{AnH}^-$ is a weaker base than ordinary phenolate anions due to the existence of intramolecular hydrogen bonds between the C-6 oxygen and the peri-amino and -hydroxy groups, as occurs in the similar case of the monoprotonated, two-electron reduction product of 1,8-dihydroxyanthraquinone.[16] The structures of $\mathbf{AnH_2}$ and $\mathbf{lAnH_2}$ have been assigned according to the following arguments: Cyclic voltammetry shows that the oxidation of $\mathbf{AnH_2}$ produces **An**, therefore, $\mathbf{AnH_2}$ is obtained through two reversible additions of protons to $\mathbf{An}^{2-}$, which creates a nitrogen–hydrogen bond and an oxygen–hydrogen bond. However, the oxidation of $\mathbf{lAnH_2}$ does not regenerate **An**, a result that indicates that the transformation of $\mathbf{AnH_2}$ into $\mathbf{lAnH_2}$ is irreversible; a tautomerism implying the replacement of a nitrogen–hydrogen bond by a carbon–hydrogen bond is likely. As is well known,[17] a mechanism involving an imine intermediary is likely for the acid-catalysed hydrolysis of a C–N bond similar to C-5-N. That is the reason why an iminium structure is ascribed to $\mathbf{LAnH_3}^+$.

In the presence of proton donors, an apparent two-electron

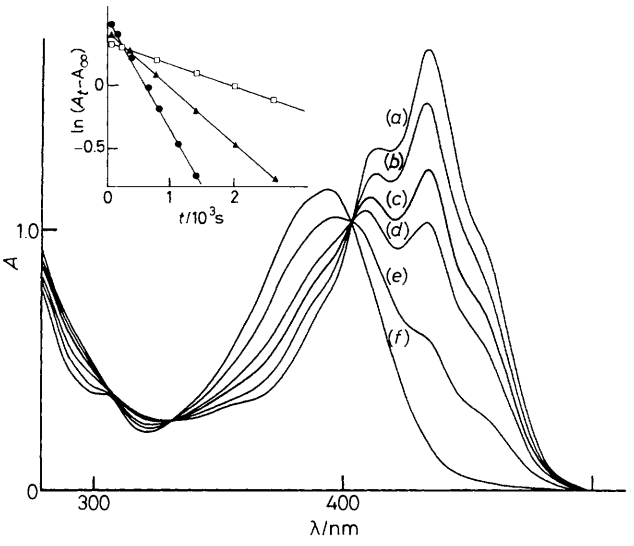

Figure 4. The kinetics of hydrolysis of 0.2 mmol dm^{-3} $\mathbf{LAnH_2}$ in aqueous 0.2 mol dm^{-3} HCl monitored spectrophotometrically at 32 °C: (*a*) 0; (*b*) 5; (*c*) 14; (*d*) 23; (*e*) 50; (*f*) 155 min (**P**). The insert shows the time dependence of the absorbance at 434 nm at various HCl concentrations: □ 0.06, ▲ 0.2, ● 1.2 mol dm^{-3}. Cell thickness: 0.5 cm.

step occurs with consecutive chemical transformation of the diprotonated reduction product $\mathbf{AnH_2}$. However, we did not observe any direct two-electron reduction of $\mathbf{AnH_2}$ and ensuing hydrogenolysis of the N–N bond (*i.e.* pyrazole D-ring opening) as was suggested in a previous polarographic study of similar anthrapyrazoles in buffered aqueous media at pH *ca.* 7.[3]

Experimental

Materials.—The anthrapyrazole anticancer agent CI-941 (hydrochloride form) (**An**) was graciously supplied by Warner–Lambert/Parke–Davis Pharmaceutical Research Division (Ann Arbor, MI). Spectrophotometric grade *N*,*N*-dimethylformamide (DMF), tetraethylammonium hydroxide (Et_4NOH) (40% solution in H_2O), triethylamine hydrochloride (TEA·HCl) and tetraethylammonium chloride (Et_4NCl) were obtained from Merck, Fluka, and Sigma respectively. Acetonitrile MeCN (from SDS) and triethylamine (TEA) (from Prolabo Commercials) were h.p.l.c. grade. Other materials were reagent grade. All chemicals were used without further purification.

General Information.—Elemental analysis was performed at the CNRS Center of Microanalysis (Gif sur Yvette). U.v.–vis. spectra were recorded on a Varian Superscan 3 spectrophotometer. Chemical-ionization (CI; NH_3) mass spectrometry (MS) was carried out on a Riber R10-10C instrument. ^1H N.m.r. (270 MHz) spectra were obtained with a Bruker WM-270 spectrometer. $SiMe_4$ was used as internal standard. All coupling constants are as those observed and are given in Hz. The assignments of the resonances were made on the basis of previous partial interpretations of spectroscopic data of a series of anthrapyrazoles,[18,19] and through the use of homonuclear decoupling experiments.

As already reported in ref. 19, difficulty was encountered in obtaining pure samples for microanalysis, particularly since the compounds tenaciously retained water and HCl. We did not dry these compounds at higher temperatures because of potential instability. The amounts of HCl and H_2O needed to rationalize the analytical data for the presence of these impurities are given in the molecular formulae.

Chromatography.—High-performance liquid chromatography (h.p.l.c.) employed a Kontron model T-414 pump, a Waters model 481 u.v.–vis. detector and a Waters Nova-Pak C_{18} stainless steel column (3.9 mm i.d. × 15 cm, 4 μm) preceded by a Waters Guard-Pak C_{18} guard column. The solvent system consisted of MeCN:H_2O (20:80, v/v containing TEA (1.4 mmol dm^{-3}), and adjusted to pH 3.2 with formic acid. A flow rate of 1.0 cm^3 min^{-1} was used and compounds were detected at 254, 394, or 460 nm. Prior to analysis by h.p.l.c., samples in DMF were filtered (Millipore FH, 0.5 μm) and diluted to a tenth concentration with the h.p.l.c. eluant. Quantities of **An** and its leuco form $\mathbf{LAnH_2}$, present in the electrolysed solution, were determined from measurements of h.p.l.c. peak heights corrected for variations in the molar absorbances among the compounds.

Preparative separations were performed by liquid column chromatography using a glass column (60 × 2.0 cm) packed with Sephadex LS-20 gel permeation resin.

Electrochemistry.—All the electrochemical experiments were carried out in DMF, since **An** is soluble in this organic aprotic solvent. In order to avoid unnecessary complications during the desalting and purification steps, the only cationic species used for the electrolysis background solutions were Et_4N^+ and $TEA{\cdot}H^+$ ions while Cl^- was the only type of anion introduced into the reaction media.

A preliminary spectrophotometric study of the acido-basic behaviour of **An** (λ_{max} 392, 470, and 498 nm) in DMF (0.1 mol dm^{-3} Et_4NCl) revealed that the deprotonation of the two ammonium groups of the side chains occurred first and simultaneously upon addition of Et_4NOH (three isosbestic points being observed at 420, 482, and 499 nm). When Et_4NOH (2.5 equiv.) were used, complete deprotonation of **An** into its neutral form (λ_{max} 375, 394, and 504 nm) could be achieved; such a solution will be referred to as a solution of neutralized **An** in DMF.*

Apparatus employed for electrochemical experiments were the same as those previously described.[20] A conventional one-compartment water-jacketed cell was used and maintained at 25 °C unless otherwise specified.

The working electrodes were a hanging mercury drop for voltammetric and chronoamperometric experiments, a gold grid located in an air-tight cell for spectroelectrochemistry,[21] and a mercury pool (*ca.* 10 cm^3) for preparative electrolyses. The auxiliary electrode was a platinum wire. For preparative electrolyses, it was fitted in a glass tube filled with a 0.1 mol dm^{-3} Et_4NCl solution in DMF. The contact was established through a medium-porosity fritted glass disk (5 mm diameter). In all electrochemical studies, the reference electrode was an aqueous KCl saturated calomel electrode (SCE) that was isolated from the bulk solution in a glass tube with a fine-porosity frit.

7-Hydroxy-5-{[2-(2-hydroxyethylamino)ethyl]amino}-2-[2(2-hydroxyethylamino)ethyl]3,4-dihydroanthra[1,9-cd]*pyrazol-6(2H)-one Dihydrochloride* ($\mathbf{LAnH_2}$). $\mathbf{LAnH_2}$ was prepared by electrochemical reduction of **An** according to the following procedure. DMF (40 cm^3) containing 0.05 mol dm^{-3} Et_4NCl and 0.05 mol dm^{-3} TEA·HCl was introduced into the one-compartment cell. After **An** (20–25 mg) (*ca.* 1.0–1.3 mmol dm^{-3}) was added and dissolved at *ca.* 32 °C (taking up to 15 min), the cell was thermostatted at 25 °C and the solution was acidified (6.3 mol dm^{-3} HCl) by addition of 21 mm^3 concentrated HCl. Controlled-potential electrolysis of the

* The ionization of the phenolic group was accompanied by a characteristic increase in absorption at 525 nm and occurred when Et_4NOH (> 3 equiv.) was added to the original solution of **An**.

resulting deaerated solution was carried out under nitrogen at −1 180 mV (*i.e.* just beyond the peak potential of peak P_{c1}) and gave a coulometric *n* value of 2.1 ± 0.1 *F* (corrected for background). When 97% of **An** had been consumed, as evidenced by h.p.l.c. analysis and absorbance measurement at 500 nm, the electrolysis was stopped; at this point a 97 ± 2% yield in leuco product **LAnH$_2$** was obtained, the impurities being the hydrolysis product **P** and the accompanying side chain. After the resulting greenish-yellow solution was concentrated on a rotary evaporator, TEA·HCl was removed by filtration and washed with cold DMF. The combined filtrates were evaporated *in vacuo* and the residue was taken up in MeOH and treated with an excess of Pr^{i}OH. The resulting pasty precipitate was collected by filtration, washed with Pr^{i}OH and subjected to column chromatography on Sephadex LH-20. Elution with the mobile phase H_2O:MeOH (85:15, v/v) adjusted to pH 2.9 with HCl yielded a large bright-yellow band, corresponding to desalted leuco product **LAnH$_2$**, which was closely followed by a small orange band due to the remaining **An**. After collection and evaporation, the former band gave **LAnH$_2$** of sufficient purity for subsequent preparation of **P**. When a higher purity was desired (assayed by h.p.l.c.), the latter chromatographic procedure was repeated twice, affording **LAnH$_2$** as a very hygroscopic orange solid: δ_H[$(CD_3)_2SO$] 3.07 (m, 4 H, 2 × CH_2CH_2OH), 3.33 (m, 6 H, C-5-NHCH$_2$CH_2, C-3-H$_2$ and C-4-H$_2$), 3.49 (m, 2 H, N-2-CH$_2$CH_2), 3.71 (m, 4 H, 2 × CH_2OH), 4.00 (m, 2 H, C-5-NHCH_2), 4.62 (t, 2 H, *J* 6 Hz, N-2-CH_2), 4.78 (br s, alcoholic OH), 6.77 (app t, 1 H, *J* 5 Hz, C-9-H), 7.49 (d, 2 H, *J* 5 Hz, C-8-H and C-10-H), 9.32–9.39 (overlapping s, 5 H, 2 × NH_2^+ and phenolic OH), 10.91 (t, 1 H, *J* 6 Hz, C-5-NH, irradiation at 4.00 gave a singlet); signals at 4.78, 7.49, and 10.91 were D_2O exchangeable. CI–MS *m*/*z* (relative abundance) 428 (*M*H$^+$, 100). u.v.–vis. (DMF), λ_{max} [ε_{max} (dm^3 mol^{-1} cm^{-1})] 462 (16 500), 437 (15 400), 412 (sh) (8 300), 354 (4 200). (Found: C, 42.6; H, 6.2; Cl, 18.2; N, 11.55. Calc. for $C_{22}H_{29}N_5O_4$·3.2 HCl 4H_2O: C, 42.87; H, 6.53; Cl, 18.45; N, 11.37%). H.p.l.c. t_R = 2 min 45 s.

6,7-*Dihydroxy*-2-[2-(2-*hydroxyethylamino*)*ethyl*]3,4-*dihydroanthra*[1,9-cd]*pyrazol*-5(2H)-*one Hydrochloride* (**P**). A solution of **LAnH$_2$** (*ca.* 10 mg) in aqueous 0.2 mol dm^{-3} HCl (40 cm^3) was heated to 32 °C until complete disappearance of the starting material, as judged by visible spectrometry. After solvent evaporation, the resulting yellow residue was subjected three times to column chromatography (Sephadex LH-20), eluting with H_2O:EtOH (80:20, v/v) adjusted to pH 2.7 with HCl. This separation procedure (*i.e.* removal of the hydrochloride salt of the aminoethylamino side chain released during the hydrolysis reaction) afforded product **P** as a brown solid, whose purity was assayed by ^{1}H n.m.r. analysis: m.p. 190–193 °C. ^{1}H N.m.r. δ_H[$(CD_3)_2SO$] 2.98 (t, 2 H, *J* 7, C-4-H$_2$), 3.09 (m, 2 H, CH_2CH$_2$OH), 3.41 (t, 2 H, *J* 7, C-3-H$_2$), 3.54 (m, 2 H, N-2-CH$_2$CH_2), 3.71 (t, 2 H, *J* 6, CH$_2$CH_2OH), 4.44 (br s, alcoholic OH), 4.71 (t, 2 H, *J* 6, N-2-CH_2), 7.07 (d, 1 H, *J* 8, C-8-H), 7.58 (t, 1 H, *J* 8, C-9-H), 7.81 (d, 1 H, *J* 8, C-10-H), 9.30 (br s, 4 H, NH_2^+ and 2 × phenolic OH); signals at 4.44 and 9.30 were D_2O exchangeable. CI–MS *m*/*z* (relative abundance) 342 (*M*H$^+$, 100). U.v.–vis. (0.2 mol dm^{-3} HCl), λ_{max} [ε_{max} (dm^3 mol^{-1} cm^{-1})], 3.94 (11 500), 306 (3 900), 256 (14 400), 245 (27 700). (Found: C, 46.75; H, 5.15; Cl, 18.3; N, 9.2. H.p.l.c. t_R 9 min 40 s. Calc. for $C_{18}H_{19}N_3O_4$, 2.4 HCl, 1.7 H_2O: C, 47.04; H, 5.03; Cl, 18.55; 9.15%).

Acknowledgements

We acknowledge support of this work by the CNRS (Unité Associée 484 'Synthèse et électrochimie des composés d'interêt pharmacologique'). J. Ughetto-Monfrin is thanked for running the mass spectra and n.m.r. spectra.

References

1 F. Arcamone, 'Doxorubicin Anticancer Antibiotics,' Academic Press, New York, 1981.
2 G. Bonadonna and S. Monfardini, *Lancet*, 1969, **1**, 837.
3 H. D. H. Showalter, D. W. Fry, W. R. Leopold, J. W. Lown, J. A. Plambeck, and K. Reszka, *Anti-Cancer Drug Design.*, 1986, **1**, 73.
4 K. Reszka, P. Kolodziejczyk, P. G. Tsoungas, and J. W. Lown, *Photochem. Photobiol.*, 1988, **47**, 625.
5 All potentials are referenced to the aqueous KCl SCE.
6 M. A. Graham, D. R. Newell, J. Butler, B. Hoey, and L. H. Patterson, *Biochem. Pharmacol.*, 1987, **36**, 3345.
7 M. Breant and G. Demange-Guerin, *Bull. Soc. Chim. Fr.*, 1969, 2935.
8 C. Amatore, M. Gareil, and J. M. Saveant, *J. Electroanal. Chem.*, 1983, **147**, 1.
9 R. S. Nicholson and I. Shain, *Anal. Chem.*, 1964, **36**, 706.
10 A. J. Kresge, *Acc. Chem. Res.*, 1975, **8**, 354.
11 W. M. Schwarz and I. Shain, *J. Phys. Chem.*, 1965, **69**, 30.
12 C. W. Greenhalgh and N. Hughes, *J. Chem. Soc. C*, 1968, 1284.
13 S. M. Bloom and R. F. Hutton, *Tetrahedron Lett.*, 1963, 1993.
14 D. J. Brand and J. Fisher, *J. Am. Chem. Soc.*, 1986, **108**, 3088.
15 M. Kikuchi, T. Yamagishi, and M. Hida, *Dyes and Pigments*, 1981, **2**, 143.
16 R. M. Wightman, J. R. Cockrell, R. W. Murray, J. N. Burnett, and S. B. Jones, *J. Am. Chem. Soc.*, 1975, **98**, 2562.
17 A. Bruylants and E. Feymants de Medicis, in 'The Chemistry of the Carbon–Nitrogen Double Bond,' ed. S. Patai, Wiley, New York, 1970, pp. 486–492.
18 H. D. H. Showalter, J. L. Johnson, and J. M. Hoftiezer, *J. Heterocycl. Chem.*, 1986, **23**, 1491.
19 H. D. H. Showalter, J. L. Johnson, J. M. Hoftiezer, W. R. Turner, L. M. Werbel, W. R. Leopold, J. L. Shillis, R. C. Jackson, and E. F. Elslager, *J. Med. Chem.*, 1987, **30**, 121.
20 A. Anne and J. Moiroux, *Nouv. J. Chim.*, 1984, **8**, 259.

Received 7th March 1989; *Paper* 9/00981G